

# ChemComm

Accepted Manuscript



This is an *Accepted Manuscript*, which has been through the Royal Society of Chemistry peer review process and has been accepted for publication.

*Accepted Manuscripts* are published online shortly after acceptance, before technical editing, formatting and proof reading. Using this free service, authors can make their results available to the community, in citable form, before we publish the edited article. We will replace this *Accepted Manuscript* with the edited and formatted *Advance Article* as soon as it is available.

You can find more information about *Accepted Manuscripts* in the [Information for Authors](#).

Please note that technical editing may introduce minor changes to the text and/or graphics, which may alter content. The journal's standard [Terms & Conditions](#) and the [Ethical guidelines](#) still apply. In no event shall the Royal Society of Chemistry be held responsible for any errors or omissions in this *Accepted Manuscript* or any consequences arising from the use of any information it contains.

## ARTICLE

# Ionic Nanoparticle Networks: Development and Perspectives in the Landscape of Ionic Liquid Based Materials

Cite this: DOI: 10.1039/x0xx00000x

Received 00th January 2012,  
Accepted 00th January 2012

DOI: 10.1039/x0xx00000x

[www.rsc.org/](http://www.rsc.org/)

Marie-Alexandra Neouze\*<sup>a</sup>, Martin Kronstein<sup>b</sup> Frederik Tielens<sup>c</sup>

This feature article gives an overview of the research performed on ionic nanoparticle networks (INN). These INN are hybrid materials consisting of inorganic nanoparticles and ionic linkers, such as imidazolium, bisimidazolium or pyridinium. The INN synthesis and properties, for catalysis or for sensoric, are presented. At each step INN materials are compared to other hybrid materials of similar composition such as ionogels or suspensions of imidazolium modified nanoparticles.

## Introduction

In the past years imidazolium based hybrid materials were intensively investigated. Indeed such inorganic-organic hybrid materials, like any hybrid materials, generate high performances by associating the features of the inorganic and organic part. The peculiarity of these imidazolium based materials arises from the versatile physico-chemical properties of the ionic organic part, consisting of imidazolium, bisimidazolium or pyridinium moieties. In this class of aromatic ionic compounds, such as imidazolium, bisimidazolium or pyridinium many possess low melting points and are referred to as ionic liquids. Ionic liquids were intensively studied owing to their broad range of interesting features. Among these features one can cite their ability to be functionalized, the possibility to tailor their ionic conductivity, thermal stability or hydrophilicity by exchanging the counter-anion. In addition they show a high ability to solubilise organic molecules as well as inorganic complexes.<sup>1,2</sup> As a consequence there are many reports on hybrid materials containing imidazolium or similar moieties. These compounds can be either entrapped in a matrix,<sup>3-6</sup> anchored,<sup>7-10</sup> or adsorbed on a surface<sup>11-14</sup> or they can be used as linker between inorganic units.<sup>15-21</sup> The corresponding inorganic part of the material could be a porous or non-porous matrix or in form of nanoparticles.<sup>4, 22-24</sup> In the resulting material, the adsorbed or attached imidazolium moiety is not liquid anymore.

Nevertheless, independently of the “state” of the moiety within the resulting material, many authors are speaking of ionic liquid based materials.

Besides the development of imidazolium based materials, researchers are devoting increasing efforts to nanoparticle networks as promising materials to make use of the collective properties of nanoparticles.<sup>25-28</sup> In this context we have developed new hybrid materials, which consists of inorganic nanoparticles covalently linked by imidazolium moieties. These are referred to as ionic nanoparticle network (INN).

The present feature article summarizes the work done on this class of materials. In addition at each step of the article, INN materials are compared with other type of ionic liquid based materials or nanoparticle networks reported in literature. The discussion will be divided as follows: (i) the synthesis of INN, by means of green chemistry process, and characterization of the networks; (ii) the processing of the material; (iii) the presentation of the catalytic properties of INN; (iv) the presentation of the thermochromic properties of INN; (v) the presentation of the luminescence feature of INN materials; (vi) the discussion of the structure of the hybrid materials.

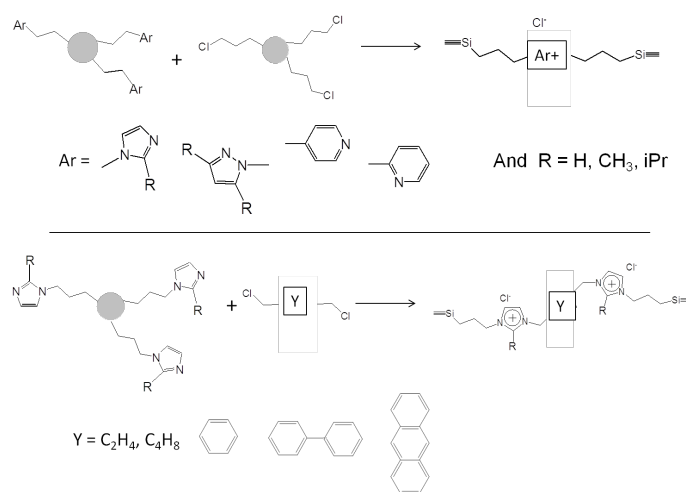
## Synthesis and characterization of Ionic Nanoparticle Networks

The INN materials were prepared by nucleophilic substitution between functional groups anchored on the surface of nanoparticles. The synthesis is divided into three steps: (i) preparation of the functional ligands and the nanoparticles; (ii) anchorage of the ligands on the surface of the nanoparticles; and finally (iii) nucleophilic substitution to link the modified nanoparticles.

For the first step various nanoparticles were prepared: silicon dioxide, titanium dioxide, zirconium dioxide, zinc oxide or silver. The oxide nanoparticles were prepared using sol-gel process, in which tetraethoxysilane, titanium isopropoxide or zirconium isopropoxide were hydrolyzed and condensed in ethanol.<sup>25</sup> In the case of silica nanoparticles the hydrolysis condensation reaction was catalyzed by ammonia.

In the second step the ligands used for functionalization of the silica nanoparticles were synthesized. These ligands are on the one hand  $\omega$ -propyltrimethoxysilanes, where  $\omega$  is an aromatic group (Ar in Scheme 1) such as pyrazole, imidazole or pyridine; and on the other hand commercially available 3-chloropropyltrimethoxysilane (Scheme 1, top) or dichloro-compounds (Scheme 1, bottom). To anchor these ligands on the nanoparticle surface they are added to the nanoparticle suspension. This suspension was stirred at room temperature overnight. For the titania nanoparticles, stable anchoring of the ligands on the surface was enabled by the use of phosphonic acid based imidazole and chlorine ligands.<sup>29, 30</sup>

In the third step the nucleophilic substitution, performed to link the nanoparticles, occurs between aromatic functionalized nanoparticles and either chloroalkyl functionalized nanoparticles (Scheme 1, top) or dichloro-molecules (Scheme 1, bottom). The reactions were performed by stirring the mixture overnight at room temperature. A turbid suspension was obtained.



**Scheme 1.** Formation of INN materials by means of nucleophilic substitution (top) between aromatic functionalized nanoparticles and chloroalkyl functionalized nanoparticles or

(bottom) between imidazole functionalized nanoparticles and dichloro-substituted compounds.

Two principal characterization methods were carried out in order to verify that the nucleophilic reaction occurred. The first method was the measurement of the thermal stability of the resulting material. Indeed, the formed ionic units, namely imidazolium, pyrazolium or pyridinium halide, present a higher thermal stability than the aromatic precursors. Indeed, the precursors starts to decompose around 120°C for the alkylhalides or 200°C for the imidazole, pyrazole or pyridine, while the INN mainly decomposes around 300°C (Figure 1, left). The first weight loss observed on the thermogravimetric analysis, below 300°C, corresponds to the elimination of adsorbed solvent, but also corresponds to some unreacted organic groups. The presence of both unreacted and non-reacted groups was investigated by <sup>15</sup>N solid state NMR.

<sup>15</sup>N solid state NMR spectroscopy gave an insight into the nitrogen environment within the material. The <sup>15</sup>N nucleus possesses a spin 1/2 but its gyromagnetic ratio and natural abundance are both notably low:  $-2.7126 \cdot 10^7 \text{ rad} \cdot \text{T}^{-1} \cdot \text{s}^{-1}$  and 0.368% respectively. Therefore the spectra were recorded under cross-polarization of the protons.<sup>31</sup> In consequence, the spectra deliver qualitative information but no quantitative results. Nevertheless, four days recording on a sample gave access to a correct spectrum where a large peak can be observed centered at 142 ppm corresponding to the imidazolium unit (Figure 1, right). A shoulder is present at the foot of the peak, associated to a chemical shift of 137 ppm which can be attributed to unreacted imidazole groups. As a matter of fact it can be concluded that most of the nitrogen containing aromatic groups did react toward their conjugated cation equivalents.

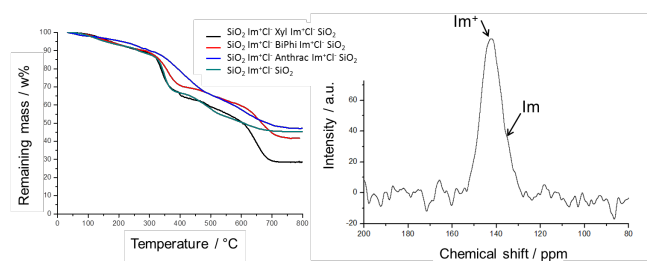


**Figure 1.** (left) TGA curves of various INN materials and (right) <sup>15</sup>N CP-MAS NMR of the INN constituting of N,N-dipropylimidazolium chloride linking silica nanoparticles.

Once the INN material is obtained, it is possible to exchange the halide anion. This anion exchange, well described for genuine imidazolium ionic liquids,<sup>32</sup> can prove the formation of the material. For this exchange, a salt of the desired anion, such as sodium tetrafluoroborate (NaBF<sub>4</sub>), potassium hexafluorophosphate (KPF<sub>6</sub>) or lithium bis(trifluoromethylsulfonyl)imide (LiN(SO<sub>2</sub>CF<sub>3</sub>)) was added to a suspension of the INN. The halide anion of the INN was thus replaced by the fluorinated anion. This replacement could be verified by detecting the halide in the solvent used for the

exchange or by the signature of the halide salts in X-ray diffraction pattern after drying (Figure 2, top). In the XRD pattern, the obtained chloride salt reflexions are marked with either a star for NaCl or a triangle for KCl. The other Bragg peaks belong to the fluorinated salt, added in large excess in order to perform the exchange.

The material is isolated by centrifugation, washed thoroughly with water, to eliminate the salts, and dried. XRD of the material shows only the amorphous signature of the amorphous silica nanoparticles, no Bragg peaks could be observed, which confirmed the complete washing of any salt, added for the exchange or formed by the exchange. The EDX analyses also showed the presence of the newly introduced anions. After exchange by tetrafluoroborate, fluorine and boron and respectively after exchange by hexafluorophosphate, phosphorous and fluorine were detected (Figure 2, bottom). It has to be noted that chlorine could still be observed after anion exchange. Its presence can have two origins, alkylchloride groups which did not react with their aromatic counterparts or chlorine ions which were not exchanged. Even though EDX analyses induce a very high incertitude on the quantification of the atoms, one can estimate the amount of exchanged anions, and thus of reacted units, at around 70 mol%.

The anion exchange on the INN materials provides first of all the possibility to tune the physic-chemical properties of the material. It was shown that the INN containing fluorinated anions were hydrophobic, while the chloride containing INN materials are hydrophilic.<sup>32</sup>

In this first part, it was shown that the synthesis of INN materials is very versatile, allowing to adapt the nature of the nanoparticle, the type of linker as well as the counter-anion at wish.

In the case of INN materials, as well as in the case of materials obtained by entrapment of ionic liquid in a matrix (so called ionogels), the simple protocol of synthesis gives access to a rich class of materials (varying the nature of the matrix entrapping on one type of ionic liquid or another etc.) The main difference lies in the exchange of the anion. For INN materials this exchange has to be performed after the synthesis while for ionogels this is not possible. The desired ionic liquid has to be prepared in a preceding step. One example of anion exchange before the preparation of an ionogel was reported by Binnemans and co-workers. There a luminescent rare-earth based anion was introduced as counter-anion.<sup>5,33</sup>

While the main advantage of preparing INN materials instead of “simply” modifying the surface of single nanoparticle with imidazolium moieties, comes from the processing aspects, as will be shown in the next paragraph.

### Processing of Ionic Nanoparticle Networks

The processing is a crucial issue in material science. One of the main differences between INN materials and other imidazolium based materials lies in the numerous possibilities to process the INN. Many different shapes could be obtained.

From INN, by slowly evaporating the solvent it is possible to obtain self-standing films, coatings or monoliths, as in the case of Ionogels. The characteristic dimensions of the objects obtained are of some tens of micrometers up to centimetres (Figure 3, top). In addition, and in contrast to Ionogels, it is also possible to make nano-lithography or layer-by-layer deposition of the INN material. The obtained objects thus have characteristic dimensions of some tens of nanometres up to some hundreds of nanometres or even micrometers (Figure 3, bottom). Considering the materials consisting of functionalized single nanoparticles reported in literature, it is also possible to make nanolithography or layer-by-layer deposition. But in addition these functionalized single nanoparticles stable suspensions could also be prepared, which is not the case for INN materials for the extended network will precipitate or form a monolith.

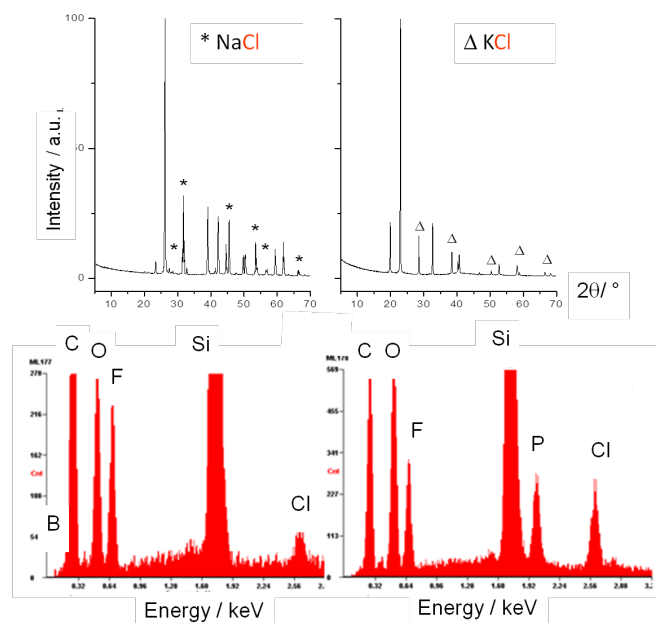


**Figure 2.** (top) XRD analyses on the exchange solvent, after separation of the material and (bottom) EDX spectra of the resulting materials.

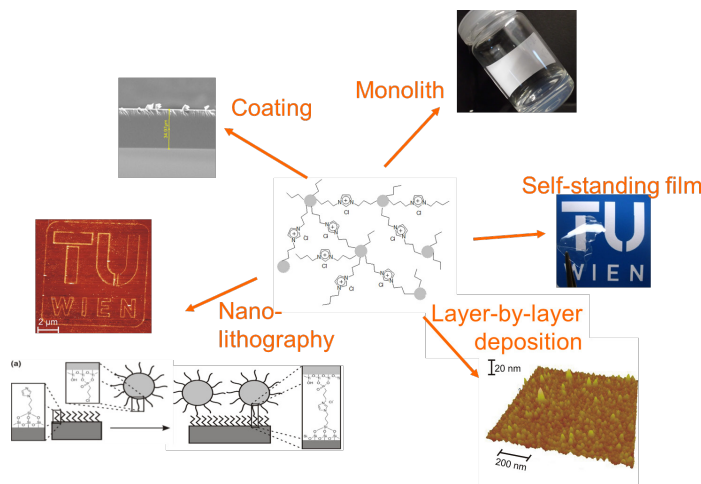


**Figure 3.** Various possibilities to process ionic nanoparticle networks.

As for any hybrid material the determination of the refractive index is not trivial. In the case of the luminescent INN (the luminescence will be discussed later on), consisting of dipropylimidazolium chloride units linking silica nanoparticles, the Raman spectrum obtained with a 632 nm laser, showed interferences (Figure 3, top left). As the thickness of the sample was known, determined by SEM cross-section imaging, the refractive index was estimated to 1.63.

With the layer-by-layer deposited material on silicon wafer, it was possible to perform lateral force microscopy (LFM) measurements (Figure 3, bottom right) in order to verify the stability of the multilayer.<sup>30</sup>

In conclusion of this short but highly important part, it is possible to state that INN materials can be processed in many different shapes, being much more versatile than the imidazolium based materials containing an inorganic counterpart. It has to be mentioned that many imidazolium-based materials were prepared using an organic polymer as matrix<sup>5, 33-39</sup> in order to improve the flexibility of the material as well as to allow an easy processing. Though, the polymeric imidazolium based materials do have limitations in the temperature range of application.

Thus, due to the presence of the silica nanoparticles the INN is a processable solid material with a direct access to the functional groups used as linkers.

### Accessibility of the functional groups in Ionic Nanoparticle Networks

The INN materials allow a direct access to the functional units linking the nanoparticles. The inter-particle spacing was investigated by means of nitrogen sorption at 77K. The INN materials contain more than 50w% of organic linkers (Figure 1, left), thus the free volume in the inter-particle spacing is quite limited.

Nevertheless, specific surface areas of up to 205 m<sup>2</sup>/g could be estimated with associated pore diameters of 2 to 15 nm for various INN materials.<sup>40</sup> We have shown that the measured porosity was enhanced in comparison with the one of genuine nanoparticles.<sup>31</sup> The percolation through the material structure is a condition for the accessibility of the functional groups. In addition, depending of the nanoparticles used to prepare the materials, various types of isotherm could be obtained. Thus, the titania based INN is characterized by a Type I isotherm due to the presence of micropores essentially. Such micropores only allow the access of very small molecules, such as air or light gas molecules in general, and are thus for example interesting for gas separation applications. While the silica based INN does solely show macroporosity, this would allow the penetration of large molecules within the network, which can be advantageous for catalytic applications. An intermediary case is the zirconia based INN, with a type IV isotherm, characteristic for mesopores.

Owing to open porosity, INN materials were investigated as catalysts for cycloaddition reaction of CO<sub>2</sub> on various epoxides.<sup>41</sup> No difference could be observed whether a monolith, a piece of gel, or a powder was used for the reaction, confirming the good accessibility of the functional groups to the reactants.

	Sample	Conversion / %	Selectivity / %
1	Blank	2.3	100
2	SiO <sub>2</sub> Im <sup>+</sup> Cl <sup>-</sup> SiO <sub>2</sub>	100	93
3	SiO <sub>2</sub> MeIm <sup>+</sup> Cl <sup>-</sup> SiO <sub>2</sub>	76	100
4	SiO <sub>2</sub> Im <sup>+</sup> Cl <sup>-</sup> BiPh Im <sup>+</sup> Cl <sup>-</sup> SiO <sub>2</sub>	100	89
5	SiO <sub>2</sub> MeIm <sup>+</sup> Cl <sup>-</sup> ZnO	88.5	76.6

**Table 1.** Conversion and selectivity after the reaction of cycloaddition with CO<sub>2</sub> pressure of 6.9 bars, a temperature of 130°C, 18 mmol of epoxide, 100 mg of material as catalyst and 4 hours reaction time.

Reactions in the presence of INN materials showed that a quantitative conversion could be reached for all the catalysts studied under relatively mild reaction conditions. The catalysts could be easily recycled for at least four runs without significant drop in conversion, but a decrease of the selectivity was nevertheless observed. The evaluation of the catalytic activity allowed a comparison of the different networks as a function of small modifications of the organic cation and/or the inorganic support. It was shown that the most active catalysts were the bis(imidazolium) silica nanoparticle networks, obtained by reaction of dichloro- precursors (Scheme 1, bottom).

Catalytic tests were also performed with INN methylated at the C2 position of the aromatic. This modification turned out to

significantly decrease the activity of the pure silica based networks. A drop in conversion of up to 25% was observed in comparison to the non-methylated analogues (Table 1). However, catalytic activity could still be observed.

Finally, the influence of the support was evaluated by replacing part of the silica nanoparticles by ZnO nanoparticles. It appeared that the partial change of support had almost no impact on the reactivity. Further optimization of the materials will now be required to improve the overall activity of these ionic nanoparticle networks.

Meanwhile, the reaction mechanism was elucidated<sup>42</sup> and it turned out that the catalytic activity is essentially driven by the anion. The variation in the catalytic activity of the various INN materials can then be related to the varying coordination strength of the halide to either the aromatic ring or the nanoparticles surface. The methylation of the C2 position of the imidazolium ring seems to slightly reduce the interaction of the chlorides with the imidazolium rings, thus inducing an increase in the conversion. Besides the better catalytic activity of the bis(imidazolium) based INN materials can be directly related to the increased amount of chloride species per milligram of material.

In conclusion, imidazolium based ionic nanoparticle networks are efficient heterogeneous catalysts for the conversion of CO<sub>2</sub> to organic cyclic carbonates. However, the catalytic activity of the INN for this kind of reaction does not differ much from other imidazolium based materials consisting on imidazolium units anchored on nanoparticles.<sup>7, 9, 10</sup> Here the main advantage of using INN materials lies in the fact that the separation of the INN is obtained by simple and rapid filtration of the medium and not by centrifugation as in the case of nanoparticle suspensions.

## Luminescence in Ionic Nanoparticle Networks

The hybrid INN materials were investigated by luminescence spectroscopy. Intense emission bands could be observed. In Figure 5 the emission spectra of various INN are presented. The first and most striking observation is that the INN can emit over a broad range of wavelength, from 300 nm up to 650 nm, with excitation wavelengths varying from 280 nm up to 470 nm.

In the case of the reference INN hybrid materials, containing a dipropylimidazolium chloride or a biphenyl bis(propylimidazolium) linker (Figure 4, A), luminescence is observed, while none of the precursors has this property originally.<sup>43</sup> Some luminescent hybrid materials containing no luminophore were already reported in literature.<sup>44-50</sup> For example, the material reported by Olive and co-workers, describes anthracene organogels.

Other INN materials were also prepared containing luminescent linkers, such as biphenyl or anthracenes (Figure 4, B and C).<sup>51</sup> For each of these materials, graphs in Figure 4, the emission of the pure imidazolium based linkers without nanoparticles was also measured for comparison (curves at the bottom of each

graph). The corresponding emission is at the bottom of each graph as it is associated to a much weaker emission than the emission of the corresponding hybrid material. Even though one has to be very careful when comparing intensities in luminescence spectroscopy, these important differences can be considered as significant. Indeed the photoluminescence spectra were measured in quartz glass cuvettes; the cuvettes were filled up to two third of their volume with a powder of the measured compound, INN materials or pure linker. As a consequence much more organic moieties were present in the cuvette in case of the pure linker. Indeed, for INN, the thermogravimetric analyses in the first part of this work showed that only half of the weight consists of the organic part, the remaining residue were silica nanoparticles. In consequence, one can state that the emission intensity of the pure linkers is indeed weaker than the one of the INN material. This observation is in agreement with the fact that pure aromatic anthracene possess a pure luminescence due to inter-particle quenching. In addition, the emission maximum of the pure linkers was never at the same wavelength as the emission maximum of the corresponding INN material.

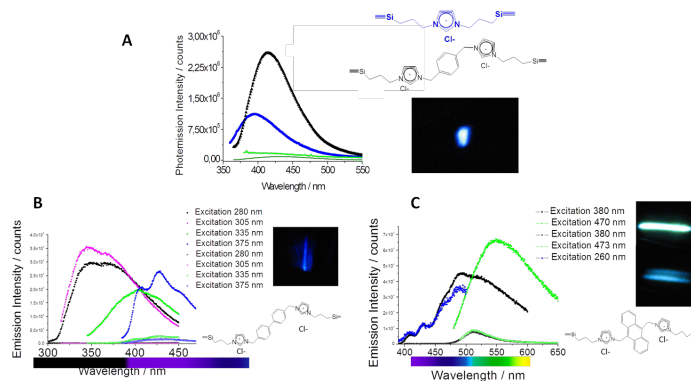


**Figure 4.** Emission spectra of various chloride based INN materials: (A) 1,3-dipropylimidazolium and xylene bis (1,3-dipropylimidazolium) with a digital photograph for an excitation at 350 nm; (B) biphenyl bis (dipropylimidazolium) with a digital photograph for an excitation at 375 nm; (C) anthracene bis (dipropylimidazolium) with digital photographs for (top) an excitation at 470 nm and (bottom) an excitation at 380 nm. On the sketches of the INN linker structure, the triple bond I standing for the link to the silica nanoparticle.

The INN hybrid materials were associated with quantum yields ranging from 10 to 26%, which are quite high values for amorphous materials containing no luminophore.

The comparison of the emission spectra of the pure linkers, either luminescent or not, and the much more intensive emission of the INN materials, leads to the conclusion that the organization of the linkers within the hybrid materials is the key to understand the origin of the luminescence. Indeed, the structuring was also pointed out to be the explanation for the other imidazolium compounds, which were reported to be luminescent, such as ionic liquid crystals.<sup>48, 52</sup> Besides, ionogels were reported to be luminescent also those not containing any luminescent precursors. These ionogels were based on entrapped butylmethylimidazolium chloride ionic liquid and

silica matrix. For the luminescent ionogels the authors proposed an explanation based on the structuring of the ionic liquid within the material. The aspect of the structuring of INN materials compared to other imidazolium containing materials will be discussed further in the last part of this work.

### Metal complexation in Ionic Nanoparticle Networks

As mentioned earlier, reactions can be performed on the counter-anion of the aromatic moiety. The reaction can be a anion metathesis as presented above, but it can also be a complexation reaction.<sup>53</sup> Here the complexation of the chloride anion was also investigated.<sup>54</sup> To this purpose  $\text{CuCl}_2$  was added to a suspension of the INN material; the progress of the complexation reaction could be monitored by its exothermic character. The transparent and translucent chloride based INN was stirred overnight and resulted in a transparent green gel, processable into a monolith or transparent coatings.

For comparison (butylmethyl)imidazolium chloride was prepared and reacted with copper dichloride to form the bis(butylmethyl)imidazolium tetrachlorocuprate moiety. This complex, which is also green, contained no inorganic nanoparticles, as opposed to the INN material.

The thermal stability of both products was investigated by TGA in air (Figure 5). It was observed that the tetrachlorocuprate complex without nanoparticles decomposed very fast starting at 180°C, while the INN material started to decompose at around 300°C. The phenomenon of thermal stabilization of a compound by introducing inorganic nanoparticles or clusters was observed in various studies, such as the stabilization of organic polymers by introducing zirconium oxo clusters.<sup>55</sup>

The increased thermal stability of the INN material in comparison to the pure bis-imidazolium tetrachlorocuprate complex allows the observation of the configuration change with temperature of the tetrachlorocuprate unit. As already described in literature, tetrachlorocuprate complexes show a transition from square planar to tetragonal under thermal activation. This configuration transition is observed directly by a colour change, thermochromism, from green, for the square planar configuration, to yellow, for the tetragonal configuration.<sup>56, 57</sup> The colour change can be observed between 180°C and 200°C for the INN material (Figure 5, top). In contrast, no colour change could be observed for the bisimidazolium tetrachlorocuprate complex without nanoparticles, due to its limited thermal stability. Indeed solely the decomposition of the compound could be observed around 180°C (Figure 5, bottom). The thermochromic behaviour of the tetrachlorocuprate INN was shown to be irreversible.

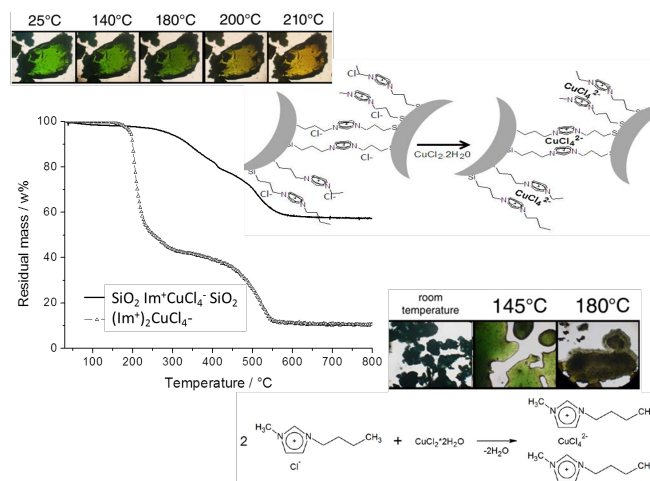


**Figure 5.** Comparative thermogravimetric analyses and digital photographs of (top) tetrachlorocuprate containing INN and (bottom) bis(butylmethyl)imidazolium tetrachlorocuprate.

As schematized in Figure 5, each copper dichloride is coordinated to two distinct imidazolium chloride units to form the tetrachlorocuprate unit. Remarkably, the chloro INN before complexation is luminescent, as described above, while after complexation the tetrachlorocuprate INN is no more luminescent. This observation is an important clue indicating that the luminescence feature of the material could arise from the organization of the aromatic ring. Thus when this organization is broken due to the copper insertion, the luminescence is no more observed.

Similar reaction was performed with  $\text{PdCl}_2$  salts added to the INN suspension. In this case, a homogeneous olive green material was obtained. The formation of  $\text{PdCl}_4^-$  anion induced the loss of luminescence.

Various groups reported the complexation reaction of various  $\text{MCl}_2$  salts among which the  $\text{CuCl}_2$  and  $\text{PdCl}_2$  salts.<sup>53, 58</sup> In the work of Iwasawa and co-workers imidazolium chloride molecules were immobilized on the surface of silica aerosol nanoparticles before performing the complexation reaction. In the article the nanoparticle suspensions with metal complex anions were used for the Kharasch catalytic reaction. The investigation of possible thermochromic effect was not mentioned.

When comparing to other ionic liquid derivatives based materials, at this stage and to the best of our knowledge no thermochromic materials were reported. Nevertheless, complexation of the anion for introducing new properties to the material was already reported. For example Bonnaffe-Moity and co-workers took advantage of the complexation ability of imidazolium species to extract uranium species.<sup>59</sup>

### Ionic Nanoparticle Networks Structure

As presented above, some of the INN properties are suggesting a strong effect of the material's organization. If the INN are amorphous toward powder X-ray diffraction, some characteristic features can be observed under small-angle X-ray diffraction (SAXS-WAXS).<sup>43</sup> On characteristic SAXS-WAXS diagrams two distinct short-range order distances can be evidenced (Figure 6, left). In order to fit these curves, a model

considering highly concentrated nanoparticles was used, which is sometimes named extended Beaucage model, suited to the investigation of objects consisting of concentrated nanoparticles.<sup>43</sup> The fitting curves, red lines in the SAXS diagram, are obtained with two distinct sets of parameters,  $d_i$  and  $\eta_i$  (characteristic distance of the ordered unit  $i$  and packing factor of this unit  $i$ ), each set being associated to one specific unit. Thus, at scattering vectors around  $0.4 \text{ nm}^{-1}$ , the oscillation can be related to the silica nanoparticles in the material, with radius of  $6.2 \text{ nm}$  confirming the values measured separately with dynamic light scattering and electronic microscopy.<sup>60</sup> The second oscillation can be observed in the range of  $4 \text{ nm}^{-1}$ . This oscillation was assigned to inter-particle units, with a characteristic length related to the length of the linker; in the case presented in Figure 7 the evaluated distance is typically  $1.37 \text{ nm}$ , whereas when the linker is xylene bisdipropylimidazolium (Figure 4, A) the distance is evaluated to be  $1.70 \text{ nm}$ .<sup>32</sup> As already mentioned, when fitting the SAXS curves, another parameter is obtained,  $\eta$ , which value informs on the efficiency of the ordering and is an expression of the intensity of the corresponding SAXS oscillation. The  $\eta$  values obtained for the INN materials, typically around  $0.3$ , corresponds to a good packing.

To obtain a better understanding of the luminescence features of the INN, the obtained results were put into correlation to the SAXS results. It turned out that, qualitatively the better the ordering of the material, the higher the quantum yield in luminescence.<sup>51</sup> Quantitatively, this SAXS/luminescence relationship could be verified when comparing the quantum yields with the packing factors  $\eta$ , as shown for three INN materials in Figure 6 (right).

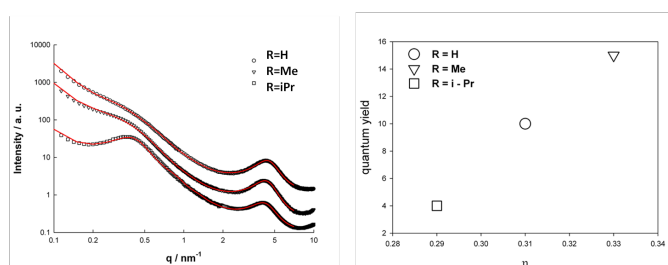


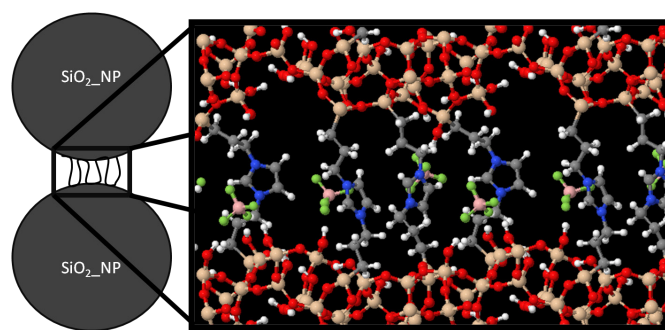
**Figure 6.** (left) SAXS diagram and corresponding fitting curves for three INN materials, based on silica nanoparticles linked by a N,N-dipropyl-alkylimidazolium, with the alkyl group being either an hydrogen, a methyl or an isopropyl group (right) evolution of the packing factor calculated from the SAXS fits versus the quantum yield measured in luminescence.

The ordering of the inter-particle space was interpreted as corresponding to  $\pi$ - $\pi$  interactions between aromatic imidazolium rings of the linker molecules.<sup>61-67</sup> In order to investigate the model at the molecular level and to determine interatomic distances DFT calculations were performed. Periodic DFR calculations (Scheme 2) on chloride dipropylimidazolium linking two flat silica slabs confirmed that the chloride anions were situated near the silica particle surface and not between the positively charged rings. The model is

based on the assumption the diameter of the nanoparticles is large enough to neglect the curvature. The silica model used represents an hydroxylated amorphous surface described earlier,<sup>68</sup> and used with success in quantum chemical studies on amorphous silica containing materials.<sup>69-76</sup>

In addition, periodic DFT calculations at the PBE level showed that the distance between two aromatic rings was small enough to allow  $\pi$ - $\pi$  interactions.<sup>74, 77</sup>

From these calculations it was possible to obtain the electron density as well as the density of states (DOS) of the material, which indicated a band gap about  $3.92 \text{ eV}$ , corresponding to a wavelength of  $316 \text{ nm}$  in case of the imidazolium chloride linker. This value obtained with silica slabs and not considering remaining pending imidazols, fits very well to the excitation wavelength of  $350 \text{ nm}$  measured for the imidazolium chloride INN (Figure 4, top).



**Scheme 2.** (left) scheme of the inter-nanoparticle spacing in INN materials and (right) DFT simulation of the nanoparticle inter-space.

Imidazolium  $\pi$ - $\pi$  interactions were often reported in literature, for example with pure ionic liquid crystals or in hybrid materials.<sup>61-65</sup> Antonietti and co-workers showed that the rings could organize, and other studies have evidences, by means of infra-red studies, that even imidazolium moieties that are no liquid crystals, could self-organize when constrained in mesopores, such as in silica ionogels,<sup>21, 78</sup> or in metal cavities.<sup>6</sup> In the case of the INN material, the “constraint” forcing the assembly of the imidazolium units comes from the anchorage onto silica nanoparticles on both sides of the linker molecule.

## Conclusions

This feature article summarized the work performed on the complex hybrid material referred as ionic nanoparticle networks (INN), consisting of a 3 dimensional network of inorganic nanoparticles covalently linked by ionic organic moieties.

First, the synthesis of the INN was presented. The synthesis pathway gives access to a large variety of INN materials when varying either the nature of the inorganic particles, or the linker or the counter-anion. The obtained INN materials can then easily be processed to monoliths, coating or self-standing films.

The original features of the INN materials were reported, namely the catalytic activity toward formation of cyclic carbonates by cycloaddition of CO<sub>2</sub> on epoxides; or the thermochromic behaviour after complexation of copper, with a green to yellow irreversible transition at 190 °C. Moreover, INN materials showed interesting luminescence properties in the visible region. Structural investigations by means of SAXS experiments have indicated a short-range order in the material arising from imidazolium  $\pi$ - $\pi$  interactions.

When compared to numerous other imidazolium based materials, it turned out that INN materials are very interesting. Indeed the thermochromic behaviour was not yet reported and the luminescence features can only be observed in specific ones, namely the ionic liquid crystals. Considering the catalytic activity, the performances of the INN are quite similar compared to other imidazolium based materials, but INN materials are much easier to separate and thus to recycle. This originates on the easy processing of the INN materials.

### Acknowledgements

The authors thank the Austrian Fonds zur Förderung der Wissenschaftlichen Forschung (FWF, Project P21190N17) as well as the Hochschuljubiläumsstiftung der Stadt Wien (grant 2007).

### Notes and references

<sup>a</sup> Institute for Materials Chemistry, Vienna University of Technology, Vienna, Austria.

<sup>b</sup> Current address: Physics of Condensed Matter, Ecole Polytechnique, Palaiseau, France; marie-alexandra.neouze@polytechnique.edu

<sup>c</sup> Université Pierre et Marie Curie, CNRS, UMR 7574, Laboratoire Chimie de la Matière Condensée, Collège de France, Paris, France

- P. Wasserscheid, T. Welton and Editors, *Ionic Liquids in Synthesis*. [In: *Ionic Liq. Synth.*, 2008; (2nd Ed.) 1], 2008.
- P. Wasserscheid, T. Welton and Editors, *Ionic Liquids in Synthesis*. [In: *Ionic Liq. Synth.*, 2008; (2nd Ed.) 2], 2008.
- R. Goebel, P. Hesemann, J. Weber, E. Moeller, A. Friedrich, S. Beuermann and A. Taubert, *Phys. Chem. Chem. Phys.*, 2009, **11**, 3653-3662.
- J. Le Bideau, L. Viau and A. Vioux, *Chem. Soc. Rev.*, 2011, **40**, 907-925.
- K. Lunstroot, K. Driesen, P. Nockemann, C. Goerller-Walrand, K. Binnemans, S. Bellayer, J. Le Bideau and A. Vioux, *Chem. Mater.*, 2006, **18**, 5711-5715.
- M.-A. Neouze and M. Litschauer, *J. Phys. Chem. B*, 2008, **112**, 16721-16725.
- B. Motos-Perez, J. Roeser, A. Thomas and P. Hesemann, *Appl. Organomet. Chem.*, 2013, **27**, 290-299.
- T. P. Nguyen, P. Hesemann and J. J. E. Moreau, *Microporous Mesoporous Mater.*, 2011, **142**, 292-300.
- Y. Xie, Z. Zhang, T. Jiang, J. He, B. Han, T. Wu and K. Ding, *Angew. Chem., Int. Ed.*, 2007, **46**, 7255-7258.
- X. Zheng, S. Luo, L. Zhang and J.-P. Cheng, *Green Chem.*, 2009, **11**, 455-458.
- B. Cosar, K. C. Icli, H. I. Yavuz and M. Ozenbas, *Electrochim. Acta*, 2013, **87**, 425-431.
- K.-M. Lee, P.-Y. Chen, C.-P. Lee and K.-C. Ho, *J. Power Sources*, 2009, **190**, 573-577.
- S. Shimano, H. Zhou and I. Honma, *Chem. Mater.*, 2007, **19**, 5216-5221.
- K. Ueno, S. Imaizumi, K. Hata and M. Watanabe, *Langmuir*, 2009, **25**, 825-831.
- P. Chevalier, R. J. P. Corriu, P. Delord, J. J. E. Moreau and M. Wong Chi Man, *New J. Chem.*, 1998, **22**, 423-433.
- R. J. P. Corriu, J. J. E. Moreau, P. Thepot and M. W. C. Man, *Chem. Mater.*, 1992, **4**, 1217-1224.
- G. Lai, J. Peng, J. Li, H. Qiu, J. Jiang, K. Jiang and Y. Shen, *Tetrahedron Lett.*, 2006, **47**, 6951-6953.
- B. Lee, H.-J. Im, H. Luo, E. W. Hagaman and S. Dai, *Langmuir*, 2005, **21**, 5372-5376.
- B. Lee, H. Luo, C. Y. Yuan, J. S. Lin and S. Dai, *Chem. Commun. (Cambridge, U. K.)*, 2004, 240-241.
- M. Litschauer and M.-A. Neouze, *J. Mater. Chem.*, 2008, **18**, 640-646.
- Y. Zhou, J. H. Schattka and M. Antonietti, *Nano Lett.*, 2004, **4**, 477-481.
- M.-A. Neouze, *J. Mater. Chem.*, 2010, **20**, 9593-9607.
- A. Taubert and Z. Li, *Dalton Trans.*, 2007, 723-727.
- M. Antonietti, D. Kuang, B. Smarsly and Y. Zhou, *Angew. Chem., Int. Ed.*, 2004, **43**, 4988-4992.
- M.-A. Neouze, *J. Mater. Sci.*, 2013, **48**, 7321-7349.
- A.-K. Herrmann, P. Formanek, L. Borchardt, M. Klose, L. Giebeler, J. Eckert, S. Kaskel, N. Gaponik and A. Eychmueller, *Chem. Mater.*, 2014, **26**, 1074-1083.
- V. Lesnyak, S. V. Voitekhovich, P. N. Gaponik, N. Gaponik and A. Eychmueller, *ACS Nano*, 2010, **4**, 4090-4096.
- A. Wolf, V. Lesnyak, N. Gaponik and A. Eychmueller, *J. Phys. Chem. Lett.*, 2012, **3**, 2188-2193.
- B. Basnar, M. Litschauer, S. Abermann, E. Bertagnolli, G. Strasser and M.-A. Neouze, *Chem. Commun. (Cambridge, U. K.)*, 2011, **47**, 361-363.
- B. Basnar, M. Litschauer, G. Strasser and M.-A. Neouze, *J. Phys. Chem. C*, 2012, **116**, 9343-9350.
- M.-A. Neouze, M. Litschauer, M. Puchberger and H. Peterlik, *Langmuir*, 2011, **27**, 4110-4116.
- M. Litschauer, M. Puchberger, H. Peterlik and M.-A. Neouze, *J. Mater. Chem.*, 2010, **20**, 1269-1276.
- K. Lunstroot, K. Driesen, P. Nockemann, K. Van Hecke, L. Van Meervelt, C. Gorller-Walrand, K. Binnemans, S. Bellayer, L. Viau, J. Le Bideau and A. Vioux, *Dalton Trans.*, 2009, 298-306.
- B. Ziolkowski, K. Bleek, B. Twamley, K. J. Fraser, R. Byrne, D. Diamond and A. Taubert, *Eur. J. Inorg. Chem.*, 2012, **2012**, 5245-5251.
- M. Armand, F. Endres, D. R. MacFarlane, H. Ohno and B. Scrosati, *Nat. Mater.*, 2009, **8**, 621-629.
- U. A. Rana, M. Forsyth, D. R. MacFarlane and J. M. Pringle, *Electrochim. Acta*, 2012, **84**, 213-222.

37. O. Winther-Jensen, S. Desai, R. L. Shepherd, P. C. Innis, B. Winther-Jensen, M. Forsyth, G. G. Wallace and D. R. MacFarlane, *Electrochem. Commun.*, 2010, **12**, 1505-1508.
38. L. D. McIntosh, T. Kubo and T. P. Lodge, *Macromolecules (Washington, DC, U. S.)*, 2014, **47**, 1090-1098.
39. M. W. Schulze, L. D. McIntosh, M. A. Hillmyer and T. P. Lodge, *Nano Lett.*, 2014, **14**, 122-126.
40. M.-A. Neouze Gauthey, M. Litschauer, M. Puchberger, M. Kronstein and H. Peterlik, *Journal of Nanoparticles*, 2013, **682945**.
41. J. Roeser, M. Kronstein, M. Litschauer, A. Thomas and M.-A. Neouze, *Eur. J. Inorg. Chem.*, 2012, **2012**, 5305-5311, S5305/5301-S5305/5302.
42. J.-Q. Wang, K. Dong, W.-G. Cheng, J. Sun and S.-J. Zhang, *Catal. Sci. Technol.*, 2012, **2**, 1480-1484.
43. M. Czakler, M. Litschauer, K. Foettinger, H. Peterlik and M.-A. Neouze, *J. Phys. Chem. C*, 2010, **114**, 21342-21347.
44. A. Getsis and A.-V. Mudring, *Z. Anorg. Allg. Chem.*, 2010, **636**, 1726-1734.
45. A. Getsis and A.-V. Mudring, *Eur. J. Inorg. Chem.*, 2011, **2011**, 3207-3213.
46. M. He, P. Huang, C. Zhang, H. Hu, C. Bao, G. Gao, R. He and D. Cui, *Adv. Funct. Mater.*, 2011, **21**, 4470-4477.
47. K. Li, J. Li, X. Cheng, W. Liu and T. Ying, *Mater. Res. Bull.*, 2011, **46**, 1113-1117.
48. A. G. L. Olive, A. Del Guerso, C. Schafer, G. Raffy and C. Giansante, *J. Phys. Chem. C*, 2010, **114**, 10410-10416.
49. S. Rodriguez-Liviano, N. O. Nunez, S. Rivera-Fernandez, J. M. de la Fuente and M. Ocana, *Langmuir*, 2013, **29**, 3411-3418.
50. R. Shahid, M. Gorlov, R. El-Sayed, M. S. Toprak, A. Sugunan, L. Kloo and M. Muhammed, *Mater. Lett.*, 2012, **89**, 316-319.
51. M. Kronstein, J. Akbarzadeh, C. Drechsel, H. Peterlik and M.-A. Neouze, *Eur. J. Inorg. Chem.*, submitted.
52. L. Douce, J.-M. Suisse, D. Guillon and A. Taubert, *Liq. Cryst.*, 2011, **38**, 1653-1661.
53. T. Sasaki, C. Zhong, M. Tada and Y. Iwasawa, *Chem. Commun. (Cambridge, U. K.)*, 2005, 2506-2508.
54. M. Kronstein, K. Kriechbaum, J. Akbarzadeh, H. Peterlik and M.-A. Neouze, *Phys. Chem. Chem. Phys.*, 2013, **15**, 12717-12723.
55. D. S. Dragan, F. R. Kogler and U. Schubert, *Polymer*, 2008, **49**, 378-385.
56. R. Bhattacharya, M. Sinha Ray, R. Dey, L. Righi, G. Bocelli and A. Ghosh, *Polyhedron*, 2002, **21**, 2561-2565.
57. R. D. Willett, J. A. Haugen, J. Lebsack and J. Morrey, *Inorg. Chem.*, 1974, **13**, 2510-2513.
58. A. Winter, K. Thiel, A. Zabel, T. Klamroth, A. Poepl, A. Kelling, U. Schilde, A. Taubert and P. Strauch, *New J. Chem.*, 2014, **38**, 1019-1030.
59. M. Bonnafe-Moity, A. Ouadi, V. Mazan, S. Miroshnichenko, D. Ternova, S. Georg, M. Sypula, C. Gaillard and I. Billard, *Dalton Trans.*, 2012, **41**, 7526-7536.
60. S. Pabisch, B. Feichtenschlager, G. Kickelbick and H. Peterlik, *Chem. Phys. Lett.*, 2012, **521**, 91-97.
61. P. Dechambenoit, S. Ferlay, B. Donnio, D. Guillon and M. W. Hosseini, *Chem. Commun. (Cambridge, U. K.)*, 2011, **47**, 734-736.
62. J. C. Diaz-Cuadros, L. Larios-Lopez, R. J. Rodriguez-Gonzalez, B. Donnio, D. Guillon and D. Navarro-Rodriguez, *J. Mol. Liq.*, 2010, **157**, 133-141.
63. A. V. Mudring, *Pacificchem 2010, International Chemical Congress of Pacific Basin Societies, Honolulu, HI, United States, December 15-20, 2010*, 2010, MATNANO-662.
64. V. Perez-Gregorio, I. Giner, M. Carmen Lopez, I. Gascon, E. Cavero and R. Gimenez, *J. Colloid Interface Sci.*, 2012, **375**, 94-101.
65. K. Tanabe, Y. Suzui, M. Hasegawa and T. Kato, *J. Am. Chem. Soc.*, 2012, **134**, 5652-5661.
66. C. G. Claessens and J. F. Stoddart, *J. Phys. Org. Chem.*, 1997, **10**, 254-272.
67. R. P. Matthews, T. Welton and P. A. Hunt, *Phys. Chem. Chem. Phys.*, 2014, **16**, 3238-3253.
68. F. Tielens, C. Gervais, J. F. Lambert, F. Mauri and D. Costa, *Chem. Mater.*, 2008, **20**, 3336-3344.
69. A. Cimasa, F. Tielens, M. Sulpizi, M.-P. Gaigeot and D. Costa, *J. Phys. Cond. Mat.*, 2014, accepted.
70. D. Costa, A. Tougeri, F. Tielens, C. Gervais, L. Stievano and J. F. Lambert, *Phys. Chem. Chem. Phys.*, 2008, **10**, 6360-6368.
71. N. Folliet, C. Gervais, D. Costa, G. Laurent, F. Babonneau, L. Stievano, J.-F. Lambert and F. Tielens, *J. Phys. Chem. C*, 2013, **117**, 4104-4114.
72. N. Folliet, C. Roiland, S. Begu, A. Aubert, T. Mineva, A. Goursot, K. Selvaraj, L. Duma, F. Tielens, F. Mauri, G. Laurent, C. Bonhomme, C. Gervais, F. Babonneau and T. Azais, *J. Am. Chem. Soc.*, 2011, **133**, 16815-16827.
73. M. M. Islam, D. Costa, M. Calatayud and F. Tielens, *J. Phys. Chem. C*, 2009, **113**, 10740-10746.
74. M.-A. Neouze, M. Kronstein, M. Litschauer, M. Puchberger, C. Coelho, C. Bonhomme, C. Gervais and F. Tielens, submitted.
75. A. Wojtaszek, I. Sobczak, M. Ziolk and F. Tielens, *J. Phys. Chem. C*, 2009, **113**, 13855-13859.
76. A. Wojtaszek, I. Sobczak, M. Ziolk and F. Tielens, *J. Phys. Chem. C*, 2010, **114**, 9002-9007.
77. M. O. Sinnokrot, E. F. Valeev and C. D. Sherrill, *J. Am. Chem. Soc.*, 2002, **124**, 10887-10893.
78. C. Fehr, P. Dieudonne, J. Primera, T. Woignier, J. L. Sauvajol and E. Anglaret, *Eur. Phys. J. E*, 2003, **12**, S13-S16.